^{99m}Tc-Interleukin-8 for Imaging Acute Osteomyelitis

Stefan Gratz, Huub J.J.M. Rennen, Otto C. Boerman, Wim J.G. Oyen, Pieter Burma, and Frans H.M. Corstens

Department of Nuclear Medicine and Section of Histomorphology, Orthopaedic Research Laboratory, University Medical Center Nijmegen, Nijmegen, The Netherlands

Early and accurate diagnosis of osteomyelitis remains a clinical problem. Acute osteomyelitis often occurs in infants and most often is located in the long bones. Radiologic images show changes only in advanced stages of disease. Scintigraphic imaging with ^{99m}Tc-methylene diphosphonate (MDP), or bone scanning, is much more sensitive in detecting acute osteomyelitis but lacks specificity. We evaluated the performance of ^{99m}Tc-interleukin-8 (IL-8) in an experimental model of acute osteomyelitis. **Methods:** Acute pyogenic osteomyelitis was induced in 10 rabbits by inserting sodium morrhuate and *Staphylococcus aureus* into the medullary cavity of the right femur. The cavity was closed with liquid cement. A sham operation was performed on the left femur. Routine radiographs were obtained just before scintigraphy. Ten days after surgery, the rabbits were divided into 2 groups of 5 animals, received an injection of either 18.5 MBq ^{111}In-granulocytes or 18.5 MBq ^{67}Ga-citrate, and were imaged both 24 h after injection and 48 h after injection. On day 12, the rabbits received either 18.5 MBq ^{99m}Tc-MDP or 18.5 MBq ^{99m}Tc-IL-8, and serial images were acquired at 0, 1, 2, 4, 8, 12, and 24 h after injection. Uptake in the infected femur was determined by drawing regions of interest. Ratios of infected femur (target) to sham-operated femur (background) (T/Bs) were calculated. After the final images were obtained, the rabbits were killed and the right femur was dissected and analyzed for microbiologic and histopathologic evidence of osteomyelitis. **Results:** Acute osteomyelitis developed in 8 of 10 rabbits. All imaging agents correctly detected the acute osteomyelitis in these animals. The extent of infection was optimally visualized with ^{67}Ga-citrate and delayed bone scanning, whereas diaphyseal photopenia was noted with both ^{99m}Tc-IL-8 and ^{111}In-granulocytes. In 1 rabbit with osteomyelitis, imaging results were falsely negative with ^{111}In-granulocytes and falsely positive with ^{99m}Tc-MDP. Quantitative analysis of the images revealed that the uptake in the infected region was highest with ^{67}Ga-citrate (4.9 $\pm$ 0.8 percentage injected dose [%ID]) and ^{99m}Tc-MDP (4.7 $\pm$ 0.7 %ID), whereas the uptake in the infected area was significantly lower with ^{99m}Tc-IL-8 (2.2 $\pm$ 0.2 %ID) and ^{111}In-granulocytes (0.8 $\pm$ 0.2 %ID) ($P < 0.0042$). In contrast, the T/Bs were significantly higher for ^{99m}Tc-IL-8 (T/B, 6.2 $\pm$ 0.3 at 4 h after injection) than for ^{67}Ga-citrate, ^{99m}Tc-MDP, and ^{111}In-granulocytes, which had ratios of 1.5 $\pm$ 0.4, 1.9 $\pm$ 0.2, and 1.4 $\pm$ 0.1, respectively ($P < 0.0001$). Radiography correctly revealed acute osteomyelitis in only 2 of 8 rabbits. **Conclusion:** In this rabbit model of osteomyelitis, ^{99m}Tc-IL-8 clearly revealed the osteomyelitic lesion. Although the absolute uptake in the osteomyelitic area was significantly lower than that obtained with ^{99m}Tc-MDP and ^{67}Ga-citrate, the T/Bs were significantly higher for ^{99m}Tc-IL-8 because of fast background clearance. The ease of preparation, good image quality, and lower radiation burden suggest that ^{99m}Tc-IL-8 may be a suitable imaging agent for the scintigraphic evaluation of acute osteomyelitis.

Key Words: acute osteomyelitis; interleukin-8; imaging infection; technetium

J Nucl Med 2001; 42:1257–1264

In cases of delayed therapy, acute osteomyelitis can, within several days, cause severe malformations of the bone that can become disabling and substantially affect the quality of life (*1*). Acute osteomyelitis usually is diagnosed on the basis of imaging, laboratory tests, and clinical examinations (*2–5*). In nuclear medicine, ^{99m}Tc-methylene diphosphonate (MDP) and ^{67}Ga-citrate are sensitive agents for the detection of osteomyelitis. Their specificity, however, is low because both agents accumulate in any area with increased bone turnover (*6*). Radiolabeled white blood cells (*7,8*) as imaging agents have a much higher specificity for scintigraphic imaging of osteomyelitis. The preparation of radiolabeled autologous white blood cells, however, is laborious and time consuming and carries a small but definite risk of personal contamination by the patients' blood and inadvertent cross-contamination between patients (*9,10*).

New radiopharmaceuticals, such as radiolabeled monoclonal antigranulocyte antibody preparations, have been proposed for easy and fast imaging of infection (*11,12*). These new agents displayed high sensitivity and specificity in patients with acute osteomyelitis (*13–15*), presumably because they act through cell-specific labeling of surface antigens as present on granulocytes.

Granulocytes are known to express interleukin-8 (IL-8) receptors abundantly (*16–19*). Therefore, the proinflammatory chemotactic cytokine IL-8 may be an interesting alternative to the current methods for imaging acute osteomyelitis.

Received Jan. 16, 2001; revision accepted Apr. 9, 2001.

For correspondence or reprints contact: Stefan Gratz, MD, Department of Nuclear Medicine, University Medical Center Nijmegen, P.O. Box 9101, 6500 HB Nijmegen, The Netherlands.

Recently, we introduced IL-8 as a new scintigraphic imaging agent. In a rabbit model with *Escherichia coli* soft-tissue infection, ^{99m}Tc-hydrazinonicotinamide-IL-8 allowed rapid visualization of the infectious foci as early as 1 h after injection, with high and rapid accretion of the radiolabel in the abscess (*20*). This study was performed primarily to gain our first preclinical experience with the use of this new ^{99m}Tc-IL-8 tracer to detect experimentally induced osteomyelitis. Therefore, we evaluated ^{99m}Tc-IL-8 as an imaging agent in a rabbit model of acute osteomyelitis. The results were compared with those obtained using the conventional and well-established agents ^{99m}Tc-MDP, ^{67}Ga-citrate, and ^{111}In-granulocytes.

MATERIALS AND METHODS

Animal Osteomyelitis Model

This study was performed in accordance with the guidelines of the local animal welfare committee. Adult female New Zealand White rabbits (weight range, 2.5–3.0 kg) were obtained from the central animal laboratory, University of Nijmegen (Nijmegen, The Netherlands), caged individually, and fed regular rabbit diet and water ad libitum. In 10 rabbits, acute osteomyelitis was induced as described previously, with minor modifications (*21–23*). The rabbits were anesthetized with a mixture of halothane, nitrous oxide, and oxygen and placed prone on the operation table. Both hind legs were shaved, disinfected with a 2% tincture of iodine, and isolated by sterile drapes. The trochanter tertius was exposed bilaterally, and the cortex was penetrated gently using a hand drill. A small syringe with a 2-mm-long silicone tube (outer diameter, 3.0 mm) was inserted into the femoral canal, and 0.5 mL 5% sodium morrhuate (QUAD Pharmaceuticals Inc., Indianapolis, IN) was inoculated in the canal. Morrhuate, a complex of fatty acids rich in arachidonic acid (*24,25*), was used to induce a local irritation. Subsequently, 0.5 mL of 5×10^6 colony-forming units of *Staphylococcus aureus* (ATCC 25923; American Type Culture Collection, Manassas, VA) was inoculated. For the sham procedure on the right femur, the canal was washed with 1 mL saline and left without a local irritation/infection procedure. Finally, both holes in the trochanter were sealed with a small amount of liquid carboxylate cement (Durelon; ESPE Dental AG, Seefeld, Germany). After polymerization of the cement, the wounds at both sides were cleaned with sterile saline solution and closed. The animals were examined regularly with special attention to wound healing, body temperature, and body weight.

Radiopharmaceuticals

^{99m}Tc-IL-8. The ^{99m}Tc-labeled IL-8 was prepared as described previously (*20*), with minor modifications. Briefly, to a 1.5-mL vial containing 6 μg IL-8 was added 0.4 mL tricine solution (*N*-[Tris(hydroxymethyl)methyl]glycine) (Fluka, Buchs, Switzerland; 100 mg/mL in 25 mmol/L succinate buffer, pH 5.0) and 0.1 mL isonicotinic acid solution (Sigma, St. Louis, MO; 20 mg/mL in 25 mmol/L succinate buffer, pH 5.0) (*26*). After the reaction mixture had been purged with a gentle stream of nitrogen, 25 μL $SnSO_4$ solution (1.0 mg/mL in 0.1N HCl) and 350 MBq $^{99m}TcO_4^-$ were added. After having been heated to 70°C for 30 min, the reaction mixture was cooled to room temperature and the radiochemical purity was determined by instant thin-layer chromatography (ITLC) on ITLC-SG strips (Gelman Laboratories, Ann Arbor, MI) with 0.1 mol/L citrate, pH 6.0, as the mobile phase.

The ^{99m}Tc-IL-8 was purified on a Sephadex G-25 column (PD-10; Pharmacia, Uppsala, Sweden) eluted with 0.5% bovine serum albumin in phosphate-buffered saline. The labeling efficiency of the ^{99m}Tc-IL-8 preparation exceeded 90%. After Sephadex G-25 purification, the radiochemical purity of the radiopharmaceutical exceeded 98% as determined by ITLC. The specific activity of the purified preparation was 50 MBq/μg (425 GBq/μmol).

^{111}In-Granulocytes. Carotid artery cannulation was performed on 1 anesthetized donor rabbit. A total of 100 mL blood was carefully drawn into acid citrate dextrose tubes (containing 7 mL acid citrate dextrose per 35 mL blood). The total leukocyte count of the donor rabbits was 6.8×10^9 cells/L, with approximately 50% granulocytes. The granulocytes were purified according to the method described by Lillevang et al. (*27*), with minor modifications (*28*). Briefly, the blood was mixed with 0.1 volume of 6% dextran (Dextran 500; Pharmacia) solution in 0.9% NaCl and allowed to settle for 1 h at room temperature. The leukocyte-rich supernatant was layered carefully on 0.3 volume of Nycoprep density medium (Nycomed, Oslo, Norway; 14.1% Nycodenz [Nycomed], 0.3% NaCl, 5 mmol/L tricine/NaOH, pH 7.2, 1.077 g/mL density, 265 mOsm) and centrifuged for 15 min at 600*g*. The plasma above the mononuclear cells, the mononuclear band, and the density medium above the granulocyte pellet were carefully removed. The pellet was washed with 5 mL Hanks' balanced salt solution (HBSS) with 10% autologous plasma and centrifuged for 10 min at 50*g*. The cell pellet was resuspended in 1.5 mL HBSS with 10% rabbit plasma. After this purification procedure, the granulocyte purity was >90%. Subsequently, 185 MBq ^{111}In-oxine were added to the cell suspension. The cells were incubated at room temperature for 30 min and centrifuged for 10 min at 50*g*. The pellet was resuspended in 5 mL cell-free autologous plasma. Labeling efficiency (cell-associated activity/total activity added) exceeded 80%. The functional integrity of the labeled granulocytes was evaluated by their in vivo performance, including transit through the lungs, as well as uptake in the liver and spleen. A dose of 18 MBq ^{111}In-oxine–labeled granulocytes was administered intravenously to each rabbit.

^{67}Ga-Citrate. ^{67}Ga-citrate (DRN 3103) was purchased from Mallinckrodt, Inc. (St. Louis, MO). A dose of approximately 18 MBq ^{67}Ga-citrate per rabbit was injected intravenously.

^{99m}Tc-MDP. A kit containing MDP and stannous chloride was labeled with ^{99m}Tc with a labeling efficiency > 95% as determined by ITLC. A dose of 18 MBq ^{99m}Tc-MDP was administered intravenously.

Receptor-Binding Assays

The receptor-binding fraction of the ^{99m}Tc-IL-8 preparation was determined in receptor-binding assays essentially as described by Lindmo et al. (*29*). For receptor-binding assays, Jurkat cells transfected with CXCR1 or CXCR2 were used (*30*). The cells were cultured at 37°C in a humidified atmosphere of air and CO_2 (95:5) in Roswell Park Memorial Institute (RPMI) 1640 medium (GIBCO, Gaithersburg, MD) containing 10% fetal calf serum, 1% glutamine, penicillin and streptomycin, 5×10^{-5} mol/L β-mercaptoethanol, and 1.5 μg/mL puromycin. Series of serially diluted cell suspension ($0.25–4 \times 10^8$ cells/mL) were incubated with 10,000 cpm of ^{99m}Tc-IL-8 in assay buffer (RPMI 1640, 0.5% bovine serum albumin, and 0.05% NaN_3). Duplicates of the lowest cell concentration were incubated in the presence of at least a

100-fold molar excess of unlabeled IL-8 to correct for nonspecific binding. After 30 min of incubation at 37°C, the cells were centrifuged (5 min, 2000*g*) and the radioactivity in the pellet (total bound radioactivity) was measured in a shielded well scintillation γ-counter (Wizard; Pharmacia). The data were graphically analyzed in a modified Lineweaver–Burk plot: a double-inverse plot of the conventional binding plot (specifically bound fraction vs. cell concentration). The receptor-binding fraction at infinite cell excess was calculated by linear extrapolation to the ordinate. The ^{99m}Tc-IL-8 preparation showed a CXCR1 receptor-binding fraction of 55% and a CXCR2 receptor-binding fraction of 45%.

Study Design

The rabbits were randomized into 2 groups: A ($n = 5$) and B ($n = 5$). The scintigraphic studies were started 10 d after induction of osteomyelitis. The radiopharmaceuticals were injected in a fixed order. On the first day of the imaging experiment, the rabbits of group A received 18.5 MBq ^{111}In-granulocytes intravenously and the rabbits of group B received 18.5 MBq ^{67}Ga-citrate intravenously. The scintigraphic images were acquired 24 and 48 h after injection of each of the radiotracers. On the third day of the imaging experiment (12 d after induction of osteomyelitis), the rabbits of group A received 18.5 MBq ^{99m}Tc-MDP intravenously and the rabbits of group B received 18.5 MBq ^{99m}Tc-IL-8 intravenously. Crossover of remaining ^{67}Ga and ^{111}In activity in the ^{99m}Tc channel was <5% as determined before and after injection of the ^{99m}Tc-labelled compounds. To exclude pharmaceutical interference with the cell-binding capacity of the radiotracer, we did not sedate the rabbits. The rabbits were immobilized in a mold and placed prone on a gamma camera equipped with a medium-energy collimator (Orbiter; Siemens Inc., Hoffman Estates, IL) for the ^{67}Ga and ^{111}In studies and with a parallel-hole, low-energy collimator for the ^{99m}Tc-MDP and ^{99m}Tc-IL-8 studies. Imaging was performed at 24 and 48 h (for ^{111}In and ^{67}Ga, respectively) after injection. The imaging sessions for ^{99m}Tc-MDP and ^{99m}Tc-IL-8 were at 3 min (blood-pool image) and 4 h (delayed image) after injection for the bone scans and at 2 min and 1, 2, 4, 8, 12, and 24 h after injection for the serial IL-8 images. Images (300,000 counts per image) were obtained and stored in a 256 × 256 matrix.

The scintigraphic results were analyzed both qualitatively and quantitatively. All scans were evaluated qualitatively without knowledge of the histopathologic outcome. Findings were considered positive if focal uptake of radioactivity at the osteomyelitic site exceeded uptake at the sham-operated site. For quantitative analysis, regions of interest were drawn over the infected right femur and the sham-operated left femur, as well as over the whole body. Additional regions of interest (at 0, 1, 4, 10, and 20 h after injection) over the lungs, liver, and spleen were drawn on the scintigrams of the rabbits that received ^{111}In-granulocytes. Counts were corrected for differences in the number of pixels before ratios and percentages were calculated. The ratios of infected femur (target) to sham-operated femur (background) (T/Bs) were calculated. Residual activity at the osteomyelitic site was determined and measured as fraction of the injected dose (whole body set to $t = 0$).

Radiologic and Histologic Analyses

The results of the scintigraphic studies were compared with the results of radiologic, microbiologic, and histopathologic examination. Conventional radiographs were obtained after the imaging sessions. While unaware of the results of all other procedures, we evaluated the radiograms with respect to 3 parameters (periosteal thinning, increased radiolucency, and inclusion of air) (*31*). Immediately after completion of the scintigraphic studies, the rabbits were killed with an overdose of sodium phenobarbital. The right femur of each animal was excised and tissue debris was removed. The femur was halved longitudinally using a high-speed dental drill with a circular metal saw. The bone cement was carefully removed. One bone specimen of each femur was sent for microbiologic examination. For histopathologic examination, the other bone specimens were fixed in 4% buffered formalin and decalcified in 10% ethylenediaminetetraacetic acid. Longitudinal sections were made, mounted on slides, and stained with hematoxylin and eosin. All sections were reviewed microscopically with respect to 3 parameters: purulent inflammation with infiltration of the bone marrow by polymorphonuclear leukocytes, necrotic bone, and bone fistulas. The presence of osteomyelitis was confirmed on the basis of these histopathologic findings.

Statistical Analysis

Mean uptake values are given as percentage injected dose (%ID) ± 1 SEM. For paired data, 1-way ANOVA using InStat software (version 3.00; GraphPad Software, Inc., San Diego, CA) was performed to compare uptake at the osteomyelitic and sham-surgery sites for the different agents. In addition, repeated-measures ANOVA was used to evaluate differences between the images acquired at different times for each agent. The level of significance was set at 0.05.

TABLE 1
Results for Group A

Rabbit no.	^{99m}Tc-MDP		^{111}In-granulocytes					
	Blood-pool image	Delayed image	24 h	48 h	Radiology	Macroscopy	Histology	Microbiology
1	++	+++	+	++	+	+++	+	+
2	+	++	+	+	−	+	+	+
3	−	++	±	±	−	—	−	−
4	+	+	±	+	−	+	+	+
5	++	++	±	+	−	+	+	+

+ = positive (+++ = complete; ++ = extensive; + = part only); − = negative; ± = equivocal; macroscopy = extension of osteomyelitis.

TABLE 2
Results for Group B

Rabbit no.	^{99m}Tc-IL-8		^{67}Ga-citrate		Radiology	Macroscopy	Histology	Microbiology
	2 h	4 h	24 h	48 h				
6	−	−	−	−	−	—	−	−
7	+	++	+	++	+	+++	+	+
8	+	++	+	++	±	+++	+	+
9	+	++	++	++	−	+	+	+
10	++	++	++	++	−	++	+	+

+ = positive (+++ = complete; ++ = extensive; + = part only); − = negative; ± = equivocal; macroscopy = extension of osteomyelitis.

RESULTS

Tables 1 and 2 summarize the observations for groups A and B, respectively. Eight of the 10 rabbits had histopathologic and microbiologic evidence of acute osteomyelitis in the right femur. Macroscopically, in 3 of 8 rabbits the osteomyelitis in the right femur had affected the complete femur, whereas in 5 of 8 rabbits the infection was apparent only in the diaphyseal and distal parts of the femur. The proximal part of the osteomyelitis-negative rabbit (rabbit 3) showed some minimal leukocytic infiltration, which was most likely caused by a local reaction to loosening of the cement. No evidence of infection was found in rabbit 6. The microbiologic studies of the bone specimens were concordant with the histopathologic findings in all infected rabbits and confirmed the presence of *S. aureus* infection in 8 of 10 rabbits. Histopathologically, the infected medullar tissue was characterized by large accumulations of polymorphonuclear leucocytes (PMNs) and some lymphocytes. Abundant areas of debris and of necrosis were seen. The trabecular bone near the growth plate was, in most cases, necrotic and infiltrated by many PMNs. The cortical bone showed necrosis and infiltration of PMNs, osteoclastic resorption, and a strong periosteal callous formation (Fig. 1). In contrast, radiologic findings were abnormal in only 2 rabbits, showing discrete periosteal thinning and increased radiolucency.

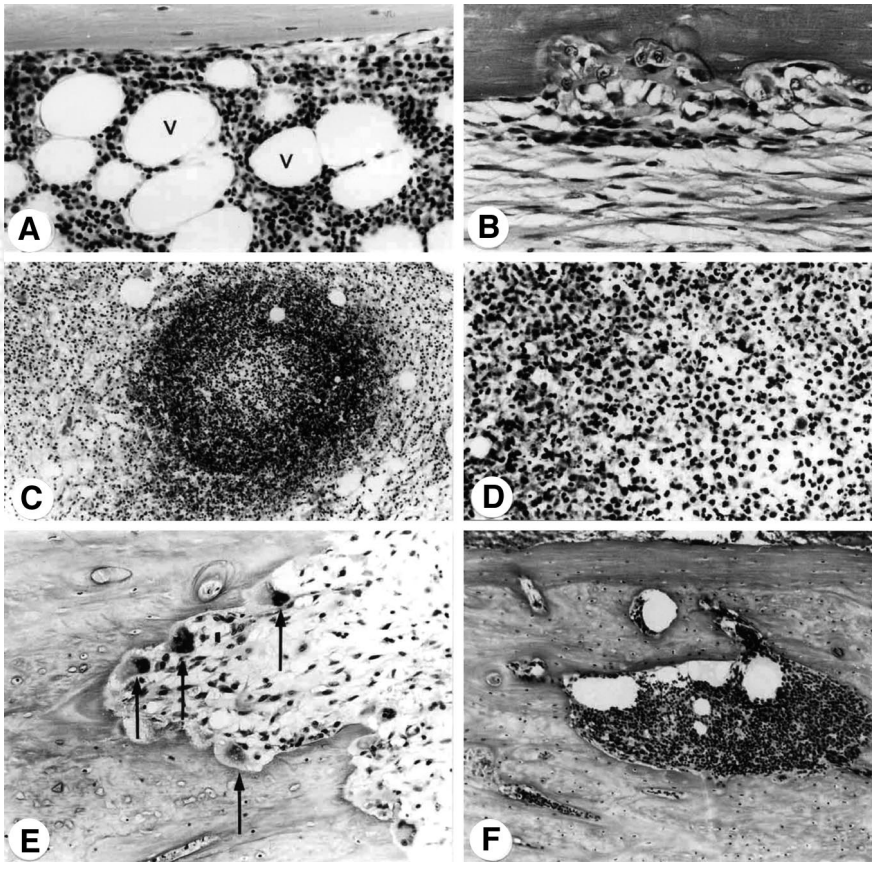

FIGURE 1. (A) Medullar tissue of control animal containing numerous fat cells (v) and red marrow (×150). (B) Medullar tissue of low-grade infection: fibrous tissue and osteoclastic erosion on endosteal surface of femoral cortex (×150). (C) Large accumulation of PMNs in medullar tissue of heavily infected bone specimen (×50). (D) Enlargement of central part because of PMN accumulation (×250). (E) Erosion channels and osteoclasts (arrows) in cortical infected bone (×100). (F) Eroded areas in cortical bone filled with leukocytes (×80).

Quantitative analysis of the scintigrams of ^{111}In-granulocytes showed rapid initial lung transit (uptake = 86 %ID at t_0 and 10 %ID at $t_{1/2}$), indicating that the labeling procedure had not affected granulocyte function (Fig. 2).

Scintigraphic analysis was performed on the images of all rabbits. Examples of the scintigraphic recordings are shown in Figure 3. All imaging agents correctly detected the acute osteomyelitis. The diaphyseal infection of the femur was best visualized with the delayed bone scan (Fig. 3, bottom, left) and, to a lesser extent, with ^{67}Ga-citrate (Fig. 3, top, right), whereas the images with ^{99m}Tc-IL-8 and ^{111}In-granulocytes were photopenic in the diaphysis. In contrast, infected areas at the proximal and distal parts of the femur were more clearly visualized with ^{99m}Tc-IL-8 and ^{99m}Tc-MDP. Equivocal results were found with ^{111}In-granulocytes in 5 animals at 24 h after injection. False-positive findings were obtained with ^{99m}Tc-MDP (rabbit 3), based on delayed images only. A fracture of the epiphyseal–metaphyseal endplate of the proximal femur was found to be radiologically responsible for the increased osteoblastic uptake. In all infected rabbits investigated, ^{99m}Tc-IL-8 scintigraphy delineated the osteomyelitic lesion as early as 2 h after injection and the quality of image improved from 2 to 4 h after injection. Uptake of ^{67}Ga-citrate and ^{111}In-granulocytes in the osteomyelitic lesions allowed detection of the infectious focus only at 48 h after injection, as shown in Figure 4.

Uptake in the osteomyelitic lesion as a fraction of the whole-body activity was significantly higher for ^{99m}Tc-MDP and ^{67}Ga-citrate than for the other 2 agents ($P < 0.005$). The bone-seeking agents ^{99m}Tc-MDP and ^{67}Ga-citrate gave similar absolute uptake at all times (up to 4.7 ± 0.7 %ID and 4.9 ± 0.8 %ID, respectively). Lower absolute uptake values were found for ^{99m}Tc-IL-8 (up to 2.2 ± 0.2 %ID) and ^{111}In-granulocytes (up to 0.8 ± 0.2 %ID). Uptake of ^{99m}Tc-IL-8 in the osteomyelitic lesion at 4 h after injection was, on average, 2.8-fold higher than that of ^{111}In-granulocytes at 48 h after injection (Fig. 4). As shown in Figure 5, the T/Bs were similar for ^{99m}Tc-MDP (1.9 ± 0.2 at 4 h after injection), ^{67}Ga-citrate (1.5 ± 0.4 at 48 h after injection), and ^{111}In-granulocytes (1.4 ± 0.1 at 48 h after injection). The T/Bs obtained with ^{99m}Tc-IL-8 increased with time up to 4 h after injection (5.0 ± 0.1 at 2 h after injection and 6.2 ± 0.3 at 4 h after injection; $P < 0.13$, not significant). For ^{99m}Tc-IL-8 at 4 h after injection, the T/Bs were 3.5-, 4.4-, and 4.7-fold higher than the T/Bs of ^{99m}Tc-MDP at 4 h after injection, ^{67}Ga-citrate at 48 h after injection, and ^{111}In-granulocytes at 48 h after injection, respectively. The mean T/B of ^{99m}Tc-IL-8 (6.2 ± 0.3 at 4 h after injection) was significantly higher than the mean T/Bs of ^{67}Ga-citrate, ^{99m}Tc-MDP, and ^{111}In-granulocytes (1.5 ± 0.4, 1.9 ± 0.2, and 1.4 ± 0.1, respectively; $P < 0.0001$).

DISCUSSION

The low diagnostic yield of radiography in this study confirmed that this technique is unreliable in establishing

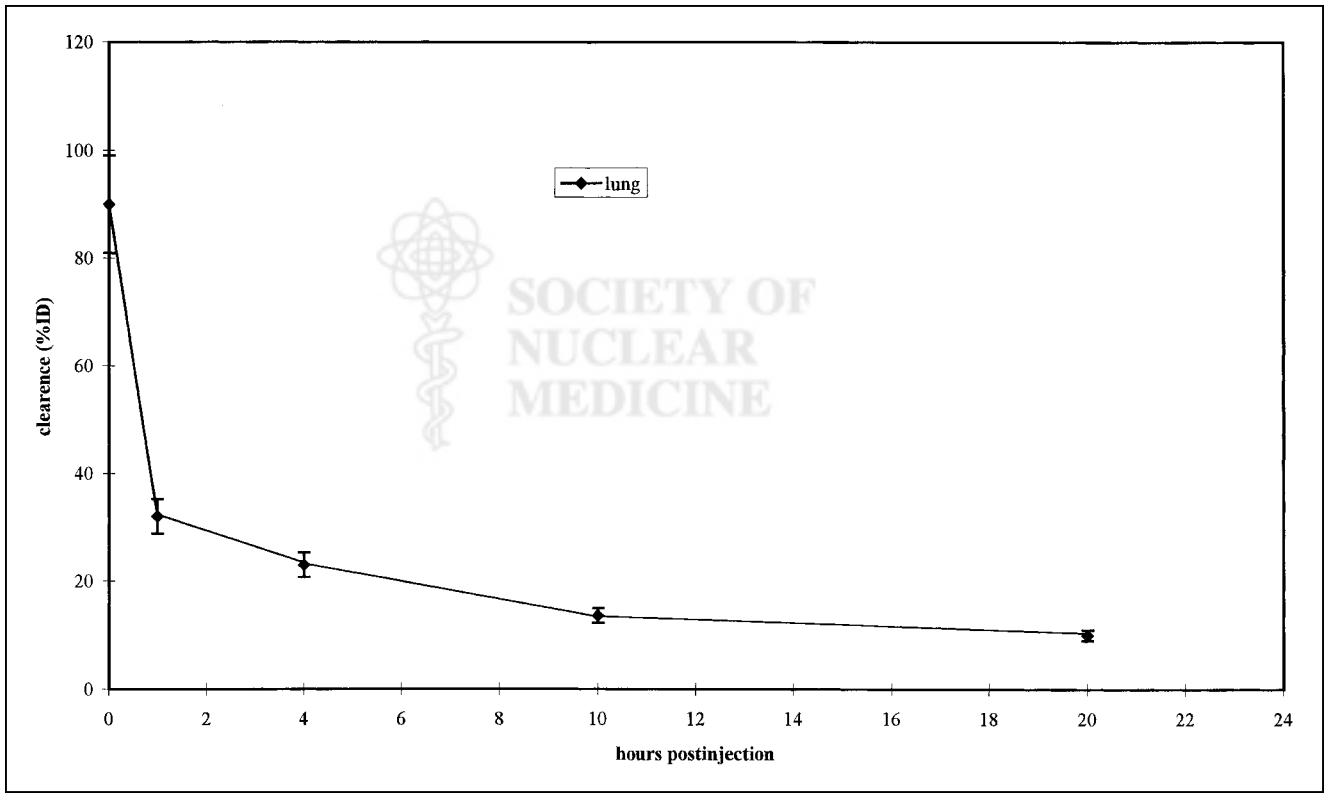

FIGURE 2. In vivo measurements of granulocyte function. Graph shows lung clearance of ^{111}In-granulocytes determined by quantitative analysis of scintigraphic images of rabbits that received ^{111}In-granulocytes. Error bars represent SEM.

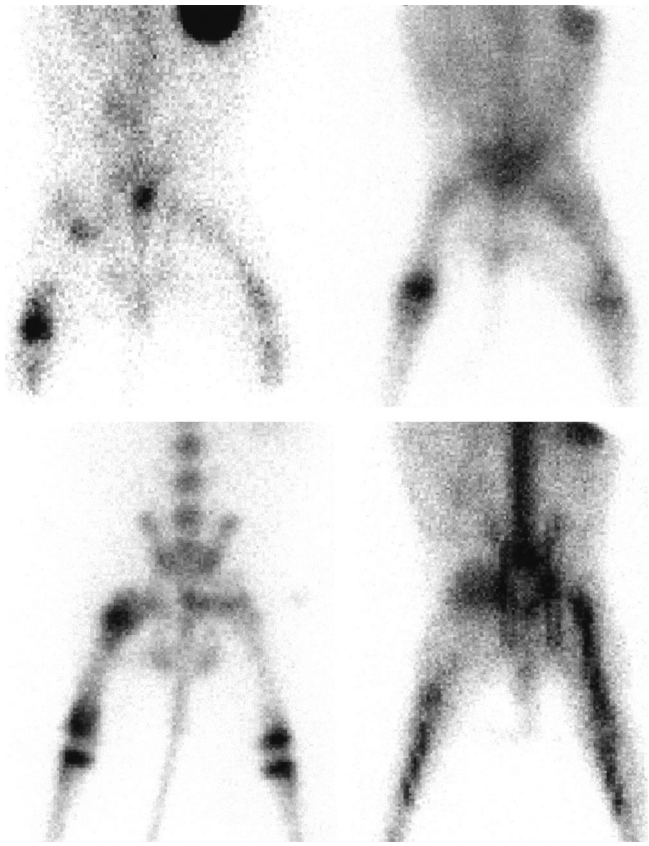

FIGURE 3. Scintigraphic images of rabbits with complete infection of femur. (Top) ^{99m}Tc-IL-8 image 4 h after injection (left) and ^{67}Ga-citrate image 48 h after injection (right) for rabbit 8 of group B. (Bottom) ^{99m}Tc-MDP image 4 h after injection (left) and ^{111}In-granulocyte image 48 h after injection (right) for rabbit 1 of group A.

acute bone infection when an additional pathologic condition is present. In osteomyelitis, the bone destruction caused by vascular ischemia, by enzymes of disintegrated polymorphs, and by increased intramedullary pressure (*32*) can be visualized with bone-seeking agents such as ^{67}Ga-citrate and ^{99m}Tc-MDP. Both radiopharmaceuticals have proven to be sensitive in detecting pathologically increased bone turnover, although the specificity of both agents is limited: other conditions may also cause increased uptake, such as tumors, activated osteoarthritis, and noninfectious inflammatory lesions (*33*). An increase in specificity can be achieved using agents targeting the neutrophils that have infiltrated the bone marrow. Up to now, these neutrophilic infiltrates have been visualized with radiolabeled leukocytes (*34*) or with radiolabeled antibodies directed against epitopes as present on granulocytes (*35*).

With ^{99m}Tc-IL-8, most infections in the rabbits were detected as early as 2 h after injection, whereas delayed 48-h postinjection images were necessary with ^{111}In-granulocytes (*36*). With ^{99m}Tc-IL-8 as well as with ^{67}Ga-citrate, all infected sites were detected, whereas delayed bone scanning alone was falsely positive in 1 rabbit and ^{111}In-granulocytes missed 1 case of osteomyelitis.

This study showed that ^{99m}Tc-IL-8, a proinflammatory chemotactic cytokine, allows visualization of osteomyelitic lesions as evidenced by infiltrated neutrophils, presumably by targeting the surface receptors on granulocytes. Furthermore, ^{99m}Tc-IL-8 performed at least as well as ^{99m}Tc-MDP and ^{67}Ga-citrate in the localization of acute bone infection.

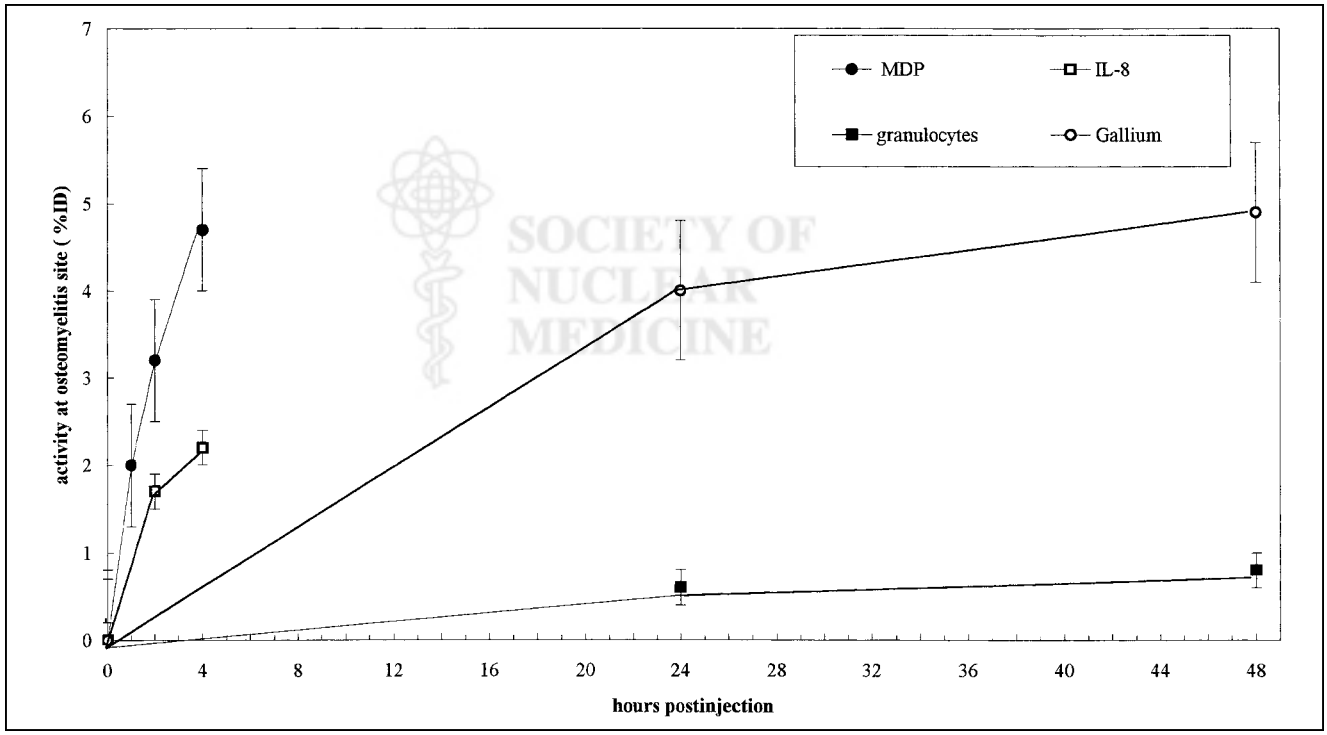

FIGURE 4. Uptake at osteomyelitic site as determined by quantitative analysis of scintigraphic images of group A rabbits administered ^{99m}Tc-MDP and ^{111}In-granulocytes and group B rabbits administered ^{99m}Tc-IL-8 and ^{67}Ga-citrate. Error bars represent SEM.

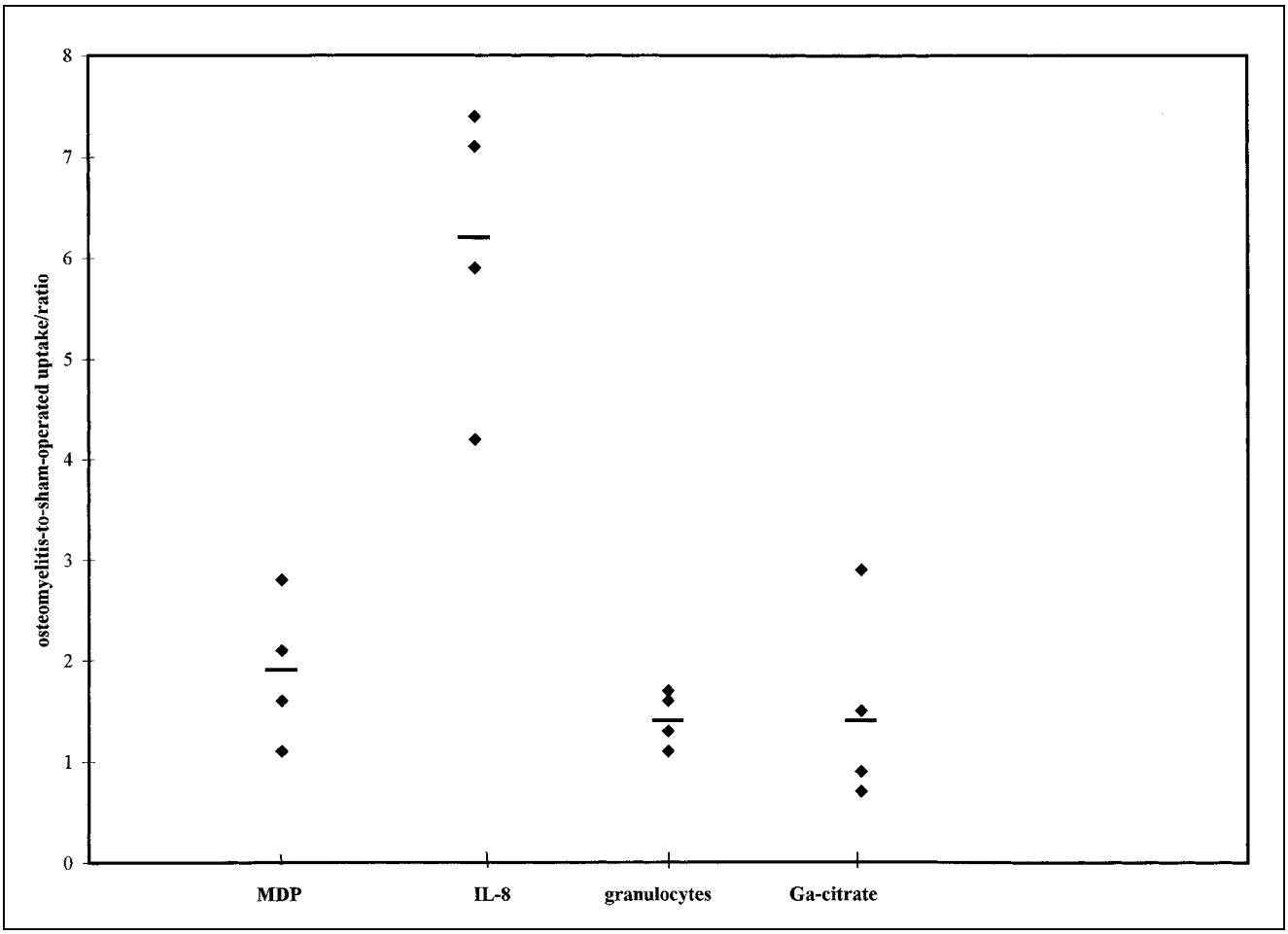

FIGURE 5. T/Bs calculated from quantitative region-of-interest analysis of scintigraphic images. Data are for 3-h (^{99m}Tc-MDP) and 48-h (^{111}In-granulocyte) images for rabbits of group A and for 4-h (^{99m}Tc-IL-8) and 48-h (^{67}Ga-citrate) images for rabbits of group B. Horizontal bars represent mean values.

Although absolute uptake of the agent in the osteomyelitic lesion was lower, the T/B obtained with ^{99m}Tc-IL-8 was highest. The direct comparison with ^{111}In-granulocytes showed superior targeting of ^{99m}Tc-IL-8.

The moderate performance of ^{111}In-granulocytes in acute osteomyelitis is in line with studies on patients with osteomyelitis (*37*). The cause of the photopenic areas in infected bones imaged with ^{111}In-granulocytes (in humans) is considered to be multifactorial and includes impaired blood supply and substitution of the bone marrow by pathologic processes. It has been documented that 14% of acute osteomyelitic lesions appear as cold lesions on scintigraphic images (*38*), most likely because subperiosteal and intraosseous pus compresses the microcirculation of the involved bone. Predominantly, this compression is thought to occur mainly in the femoral diaphysis and femoral head (*39*).

Granulocytes abundantly express IL-8 receptors (*16–19*) on their cell membrane. Moreover, IL-8 and tumor necrosis factor are locally produced by inflammatory cells in the bone marrow and play an important role in the attraction of neutrophils, which may result in a further increase in IL-8 receptor–positive cells in the infectious focus (*1*). The data in this study suggest that ^{99m}Tc-IL-8 is more suited than ^{111}In-granulocytes for imaging osteomyelitis, presumably because infiltration of the radiolabeled granulocytes is hampered by the physiologic factors mentioned above (*40*).

The absolute uptake of MDP in the femur in the instance of false positivity (rabbit 3) was as high as 2.3 %ID and in the same range as the osteomyelitic cases, illustrating the increased uptake of ^{99m}Tc-MDP in any site of bone repair of any cause. Similarly, with ^{67}Ga-citrate both the absolute uptake and the T/B were similar to those obtained with ^{99m}Tc-MDP. The values of the absolute uptakes in the infected bone were lower for ^{99m}Tc-IL-8 than for the bone-seeking agents, but the T/Bs were 4.7-fold higher for ^{99m}Tc-IL-8 than for the others. This finding indicates that there was no falsely positive uptake at the sham-surgery site and that ^{99m}Tc-IL-8 uptake increased at the infected site over time while the background activity decreased.

CONCLUSION

In this study, ^{99m}Tc-IL-8 accurately revealed acute osteomyelitis in a rabbit model. ^{99m}Tc-IL-8 correctly identified all rabbits with acute osteomyelitis within 4 h after injection. The ease of preparation, early good image quality, and lower radiation burden suggest that ^{99m}Tc-IL-8 may be a suitable imaging agent for the scintigraphic evaluation of acute osteomyelitis.

ACKNOWLEDGMENTS

The authors thank Gerry Grutters and Henny Eikholt (Central Animal Laboratory, University of Nijmegen) for expert assistance with the animals, Emile Koenders (Department of Nuclear Medicine, University Medical Center Nijmegen) for excellent technical assistance, and Drs. Pius Loetscher and Marco Baggiolini (Theodor Kocher Institute, University of Bern, Bern, Switzerland) for the kind gift of the cell lines. This study was supported in part by the Deutsche Forschungs Gesellschaft.

REFERENCES

1. Lew DP, Waldvogel FA. Osteomyelitis. *N Engl J Med.* 1997;336:999–1007.
2. David R, Barron BJ, Madewell JE. Osteomyelitis, acute and chronic. *Radiol Clin North Am.* 1987;25:1171–1201.
3. Ram PC, Martinez S, Korobkin M, Breiman RS, Gallis HR, Harrelson JM. CT detection of intraosseous gas: a new sign of osteomyelitis. *AJR.* 1981;137:721–723.
4. Morrison WB, Schweitzer ME, Batte WG, Radack DP, Russel KM. Osteomyelitis of the foot: relative importance of primary and secondary MR imaging signs. *Radiology.* 1998;207:625–632.
5. Rifai A, Nyman R. Scintigraphy and ultrasonography in differentiating osteomyelitis from bone infarction in sickle cell disease. *Acta Radiol.* 1997;38:139–143.
6. Gratz S, Doerner J, Oestmann JW, et al. ^{67}Ga-citrate and 99Tcm-MDP for estimating the severity of vertebral osteomyelitis. *Nucl Med Commun.* 2000;21:111–120.
7. Joseph K, Damann V, Engeroff G, Gruner KR. Labeling of leukocytes with ^{99m}Tc-HMPAO: first clinical results [in German]. *Nucl Compact.* 1986;17:277–283.
8. Schauwecker DS. Osteomyelitis: diagnosis with In-111-labeled leukocytes. *Radiology*. 1989;171:141–146.
9. Rojas-Burke J. Health officials reacting to infection mishaps. *J Nucl Med*. 1992;33:13N–14N, 27N.
10. Kaim A, Maurer T, Ochsner P, Jundt G, Kirsch E, Mueller-Brand J. Chronic complicated osteomyelitis of the appendicular skeleton: diagnosis with technetium-99m labelled monoclonal antigranulocyte antibody-immunoscintigraphy. *Eur J Nucl Med.* 1997;24:732–738.
11. Becker W, Goldenberg DM, Wolf F. The use of monoclonal antibodies and antibody fragments in the imaging of infectious lesions. *Semin Nucl Med.* 1994;24:142–153.
12. Becker W, Borst U, Fischbach W, Pasurka B, Schafer R, Borner W. Kinetic data of in-vivo labeled granulocytes in humans with a murine Tc-99m-labelled monoclonal antibody. *Eur J Nucl Med*. 1989;15:361–366.
13. Becker WS, Saptogino A, Wolf FG. The single late 99Tcm granulocyte antibody scan in inflammatory diseases. *Nucl Med Commun*. 1992;13:186–92.
14. Becker W, Bair J, Behr T, et al. Detection of soft-tissue infections and osteomyelitis using a technetium-99m-labeled anti-granulocyte monoclonal antibody fragment. *J Nucl Med*. 1994;35:1436–1443.
15. Holmes WE, Lee J, Kuang WJ, Rice GC, Wood WI. Structure and functional expression of a human interleukin-8 receptor. *Science.* 1991;253:1278–1280.
16. Lange JM, Boucher CA, Hollak CE, et al. Failure of zidovudine prophylaxis after accidental exposure to HIV-1. *N Engl J Med.* 1990:10;322:1375–1377.
17. Murphy PM, Tiffany HL. Cloning of complementary DNA encoding a functional human interleukin-8 receptor. *Science.* 1991;253:1280–1283.
18. Lee J, Horuk R, Rice GC, Bennett GL, Camerato T, Wood WI. Characterization of two high affinity human interleukin-8 receptors. *J Biol Chem.* 1992;267:16283–16287.
19. Cerretti DP, Kozlosky CJ, Vanden Bos T, Nelson N, Gearing DP, Beckmann MP. Molecular characterization of receptors for human interleukin-8, GRO/melanoma growth-stimulatory activity and neutrophil activating peptide-2. *Mol Immunol.* 1993;30:359–367.
20. Rennen HJJM, Boerman OC, Oyen WJG, van der Meer JWM, Corstens FHM. Specific and rapid scintigraphic detection of infection with Tc-99m-labeled interleukin-8. *J Nucl Med.* 2000;42:117–123.
21. O'Reilly T, Kunz S, Sande E, Zak O, Sande MA, Tauber MG. Relationship between antibiotic concentration in bone and efficacy of treatment of staphylococcal osteomyelitis in rats: azithromycin compared with clindamycin and rifampin. *Antimicrob Agents Chemother*. 1992;36:2693–2697.
22. Nelson DR, Buxton TB, Luu QN, Rissing JP. An antibiotic resistant experimental model of Pseudomonas osteomyelitis. *Infection*. 1990;18:246–248.
23. Mader JT, Wilson KJ. Models of osteomyelitis. In: Zak O, Sande MA, eds. *Experimental Models in Antimicrobial Chemotherapy*. Vol 2. London, U.K.: Academic Press; 1986:155–173.
24. Rissing JP, Buxton TB, Weinstein RS, Shockley RK. Model of experimental chronic osteomyelitis in rats. *Infect Immun*. 1985;47:581–586.
25. Henry NK, Rouse MS, Whitesell AL, McConnell ME, Wilson WR. Treatment of methicillin-resistant Staphylococcus aureus experimental osteomyelitis with ciprofloxacin or vancomycin alone or in combination with rifampin. *Am J Med*. 1987;82:73–75.
26. Liu S, Edwards DS, Harris AR. A novel ternary ligand system for ^{99m}Tc-labeling of hydrazino-nicotinamide-modified biologically active molecules using imine-N-containing heterocycles as coligands. *Bioconjug Chem.* 1998;9:583–595.
27. Lillevang ST, Toft P, Nilsen B. A method for isolating granulocytes from rabbit blood without causing activation. *J Immunol Methods*. 1994;28;169:137–138.
28. Böyum A, Lövhaug D, Tresland L, Nordlie EM. Separation of leucocytes: improved cell purity by fine adjustments of gradient medium density and osmolality. *Scand J Immunol.* 1991;34:697–712.
29. Lindmo T, Boven E, Cuttitta F, Fedorko J, Bunn PA Jr. Determination of the immunoreactive fraction of radiolabeled monoclonal antibodies by linear extrapolation to binding at infinite antigen excess. *J Immunol Methods*. 1984;72:77–89.
30. Alvarez-Gonzalez R, Eichenberger R, Loetscher P, Althaus FR. A new highly selective physicochemical assay to measure NAD+ in intact cells. *Anal Biochem*. 1986;156:473–480.
31. David R, Barron BJ, Madewell JE. Osteomyelitis, acute and chronic. *Radiol Clin North Am*. 1987;25:1171–1201.
32. Kahn DS, Pritzker KP. The pathophysiology of bone infection. *Clin Orthop*. 1973;96:12–19.
33. Modic MT, Feiglin DH, Piraino DW, et al. Vertebral osteomyelitis: assessment using MR. *Radiology.* 1985;157:157–166.
34. Peters AM, Saverymuttu SH, Reavy HJ, Danpure HJ, Osman S, Lavender JP. Imaging of inflammation with indium-111 tropolonate labeled leukocytes. *J Nucl Med*. 1983;24:39–44.
35. Joseph K, Höffken H, Bosslet K, Schorlemmer HU. Imaging of inflammation with granulocytes labelled in vivo. *Nucl Med Commun*. 1988;9:763–769.
36. Oyen WJ, Claessens RA, van-Horn JR, van-der-Meer JW, Corstens FH. Scintigraphic detection of bone and joint infections with indium-111-labeled nonspecific polyclonal human immunoglobulin G. *J Nucl Med.* 1990;31:403–412.
37. Mok YP, Carney WH, Fernandez-Ulloa M. Skeletal photopenic lesions in ^{111}In-WBC imaging. *J Nucl Med.* 1984;25:1322–1326.
38. Datz LF, Thorne DA. Cause and significance of cold bone defects on indium-111-labeled leukocyte imaging. *J Nucl Med.* 1987,28:820–823.
39. Athens JW, Haab OP, Raab SO. Leukokinetic studies: the total blood, circulating and marginal granulocyte pools and granulocyte turnover rate in normal subjects. *J Clin Invest.* 1961;40:989–995.
40. Weiblein BJ, Forstrom LA, McCullough J. Kinetics of In-111-labelled granulocytes. *J Lab Clin Med.* 1979;94:246–255.